

Passivity Analysis for Flexible Multilink Space Manipulators

Christopher J. Damaren*

Royal Roads Military College, FMO Victoria, British Columbia V0S 1B0, Canada

The important input-output property of passivity is explored for a general flexible space manipulator with chain topology. The manipulator is assumed to consist of rigid and/or flexible links interconnected via revolute joints, and a free rigid spacecraft and cantilevered payload are modeled at the base and tip, respectively. Actuation on the spacecraft and torques at the joints serve as control inputs and a suitably modified input variable is constructed. The notion of reflected tip position introduced by Wang and Vidyasagar for a single flexible link is extended to the multilink case and used to define a corresponding modified output variable. The dynamics governing the system are developed using a Lagrangian approach and both linearized and nonlinear forms of the mapping relating modified inputs to modified outputs are examined. Our major result shows that the transfer function in the linear case is positive real when the spacecraft and payload are much more massive than the manipulator links. The corresponding nonlinear analysis shows that the mapping is, in fact, passive and uncovers an approximate static relationship between the elastic coordinates and applied torques. A numerical example employing the Space Shuttle, remote manipulator system, and payload is used to demonstrate the validity of the theoretical results. Applications to control system design are indicated.

I. Introduction

COLLOCATION of sensors and actuators has played an important role in the control of flexible structures. It is well known that the transfer matrix relating collocated force (torque) actuators to translational rate (angular rate) sensors is positive real (PR).¹ Hence, by one form of the passivity theorem, any strictly positive real (SPR) compensator will stabilize the system. It is important to note that the property of positive realness holds regardless of modal uncertainty and the number of modeled vibration modes.^{2,3} Hence, the stability of the closed-loop system is robust with respect to uncertainty in these quantities. Although PR and SPR are terms usually restricted to linear, time-invariant systems, their generalizations, passivity and strict passivity, can be used to establish stability for nonlinear systems. For robot manipulators modeled as chains of rigid bodies, it is known that the forward dynamics map from joint torques to joint rates (assuming revolute joints) is passive.⁴ In this situation, passivity stems from the inherent collocation and cannot be defeated by the configuration dependence of the mass matrix. Hence, any strictly passive feedback controller will stabilize the system. This is one way of establishing the stability provided by joint-space proportional-derivative control. Plants which satisfy a passivity constraint are also amenable to model reference adaptive control techniques.^{4,5}

Space manipulators are characterized by large, lightweight members which exhibit significant structural flexibility. Vibration suppression of the Shuttle remote manipulator system (RMS) will be beneficial to space station subassembly,⁶ and it will be necessary for fast, accurate tracking of the next generation of space manipulators. One of the challenges posed by these structures is control of both joint and elastic motion with fewer actuators than degrees of freedom. For structurally flexible robot arms, the passivity of the dynamics relating joint torques to joint rates can still be established which will emerge as a special case of the results presented here. However, this is a less useful result since the end-effector motion depends on the elastic deformations as well. The inherent noncollocation between joint-based torque actuation and the end-effector motion has long been noted as the basic problem in control of these structures. In fact, it has been pointed out that in the case of a single

flexible link, the transfer function relating joint torque to tip velocity is nonminimum phase⁷ and hence cannot be PR.

Given the desirability of the passivity property, some research has concentrated on modifying the input and/or output of systems so as to realize this property.^{8–11} For example, Wang and Vidyasagar¹⁰ have introduced the notion of reflected tip position for a single flexible link. They viewed the tip position as being the sum of a rigid contribution from the joint angle and an elastic contribution stemming from the tip deflection. They defined the reflected tip position as the rigid portion less the elastic part and showed numerically that the transfer function from root torque to reflected tip rate is passive. This was rigorously demonstrated by Pota and Vidyasagar¹¹ using the properties of the pinned-free modes of the link. The extension to the case with hub inertia has been treated,¹² and passivity over a range of frequencies was demonstrated for a sufficiently stiff link.

Although a single pinned flexible beam is a useful starting point, it does not exhibit many of the complex characteristics of flexible multilink manipulators operating in space. These include multiple inputs and outputs, coupling to the spacecraft dynamics, and configuration-dependent mass matrices. In this work, we extend the concept of reflected tip position to a general flexible space manipulator. It is assumed to be hinged to a free rigid spacecraft and a rigid payload is cantilevered at the end effector. Our main result follows from assuming that the masses of the spacecraft and payload are much greater than those of the individual links. This assumption is not unduly restrictive for many manipulation scenarios in the space environment. It is shown that in this asymptotic situation, the mapping relating special inputs and outputs is passive.

In Sec. II, we develop the motion equations using a Lagrangian approach with an emphasis on the kinematics describing the spacecraft and payload velocities. These are subsequently linearized in Sec. III, and the mode shapes are examined. The transfer function relating suitably modified inputs and outputs is developed and shown to be positive real for special outputs under the massive spacecraft and payload assumption. Key ideas borrowed from the single link analysis are the notion of tip reflection and the use of unconstrained vibration modes. Although this result holds for the linearized form of the motion equations, the extension to the nonlinear setting is tackled in Sec. IV. A byproduct of this approach is an approximate static relationship relating the applied torques to the elastic coordinates. Although the linear results are subsumed by the nonlinear analysis, the former approach yields much insight into the structure of the motion equations and the vibration modes. A numerical demonstration of the results is provided in Sec. V for a model of the Space Shuttle, the remote manipulator system, and a payload. The results fully support the theoretical analyses. Applications to

Received Aug. 3, 1993; revision received April 18, 1994; accepted for publication Aug. 9, 1994. Copyright © 1994 by the American Institute of Aeronautics and Astronautics, Inc. All rights reserved.

*Associate Professor, Department of Engineering, currently Senior Lecturer, Department of Mechanical Engineering, University of Canterbury, Private Bag 4800, Christchurch, New Zealand. Member AIAA.

control system design and an indication of future directions are provided.

II. Equations of Motion

The following development is restricted to a chain of bodies, $\{B_0, \dots, B_{N+1}\}$, as shown in Fig. 1. We locate a reference frame \mathcal{F}_n in B_n which in the case of the manipulator links, $n = 1, \dots, N$, is assumed to coincide with the inboard articulation point, O_n . The links are taken to be rigid or flexible and interconnected with single-DOF revolute joints. B_0 is a free spacecraft which is modeled as a rigid body and cantilevered to the end of B_N is a rigid payload, B_{N+1} . Hence, its body-fixed frame \mathcal{F}_{N+1} locates the end effector.

The generalized Cartesian position of the spacecraft, $\rho_0(t)$, is described relative to an inertial frame \mathcal{F}_I . The vector $\rho_0(t)$ is a six-tuple whose upper half consists of the position coordinates R_0 and whose bottom half contains three integrable attitude coordinates (i.e., Euler angles) parameterizing the rotation matrix C_{0I} . The joint angles are $\theta_n(t)$, $n \in [1, N]$, $\theta \triangleq \text{col}\{\theta_n(t)\}$, and the elastic deflections $u_{n,e}$ are discretized using shape functions $\psi_{n\alpha}$ that satisfy cantilevered boundary conditions at O_n :

$$u_{n,e}(r, t) = \sum_{\alpha=1}^{s_n} \psi_{n\alpha}(r_n) q_{n\alpha}(t), \quad q_{n,e} \triangleq \text{col}\{q_{n\alpha}\} \quad (1)$$

The ensemble of elastic coordinates describing the flexible deformations will be designated $q_e(t) \triangleq \text{col}\{q_{n,e}\}$. In the sequel, a Lagrangian approach will be employed with generalized coordinates

$$q \triangleq \text{col}\{\rho_0, \theta, q_e\} \quad (2)$$

and it will be demonstrated that the motion equations are of the standard second-order form.

Kinematics

The notational framework follows that of Sincarsin and Hughes¹³ and Hughes and Sincarsin.¹⁴ The absolute velocity v_n and angular velocity ω_n of the inboard articulation point of B_n , O_n , are expressed in \mathcal{F}_n . They are collected into a single generalized velocity vector $v_n \triangleq \text{col}\{v_n, \omega_n\}$ which is a 6×1 column matrix. The kinematical relationship governing the generalized velocities can be written recursively as¹³

$$v_{n+1} = T_{n+1,n} v_n + S_{n+1,n} \dot{q}_{n,e} + P_{n+1} \dot{\theta}_{n+1} \quad (3)$$

$$T_{n+1,n} \triangleq \begin{bmatrix} C_{n+1,n} & -C_{n+1,n} \hat{r}_{n,n+1}^* \\ \mathbf{0} & C_{n+1,n} \end{bmatrix}$$

Here, $C_{n+1,n}(\theta_{n+1}, q_{n,e})$ denotes the rotation matrix from \mathcal{F}_n to \mathcal{F}_{n+1} , $\hat{r}_{n,n+1}(q_{n,e})$ is the deformed position of \mathcal{F}_{n+1} with respect to \mathcal{F}_n (expressed in the latter frame), and P_{n+1} is a projection matrix which aids in expressing the generalized velocity induced by the joint motion. Complete descriptions of the matrices $C_{n+1,n}$ and $S_{n+1,n}$ which encompass nonlinear elastic effects are given in Ref. 15. Given the assumption of single-DOF rotational joints, P_n is a constant 6×1 vector for $n \in [1, N]$. For future reference, the generalized velocities of the manipulator links will be collected together: $v_\ell = \text{col}\{v_n\}$, $n = 1, \dots, N$.

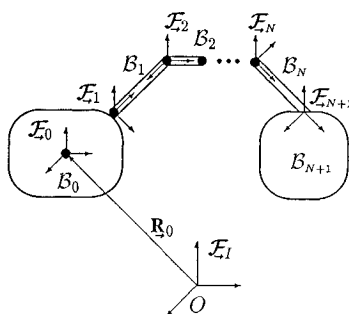


Fig. 1 Spacecraft—manipulator—payload system.

For B_0 , we shall express the generalized velocity as

$$v_0 = P_0(\rho_0) \dot{\rho}_0 \quad (4)$$

where $\rho_0(t)$ has been described earlier. Hence, $P_0 = \text{diag}\{C_{0I}(\rho_0), E_{0I}(\rho_0)\}$ where E_{0I} is the configuration-dependent matrix mapping Euler rates into angular velocity. For the case $n = -1$, Eq. (3) is valid provided $P_{n+1} \dot{\theta}_{n+1}$ is replaced with $P_0 \dot{\rho}_0$. For the payload, we take $P_{N+1} = \mathbf{0}$ and make the identification $v_t \equiv v_{N+1}$ where t connotes tip. We further define the Jacobian-type matrices

$$\begin{aligned} \hat{T}_0 &= \text{col}\{T_{n0} P_0\}, & \hat{T}_\theta &= \text{matrix}\{T_{nm} P_m\} \\ \hat{T}_e &= \text{matrix}\{T_{n,m+1} S_{m+1,m}\} \\ \hat{J}_0 &= T_{N+1,0} P_0, & \hat{J}_\theta &= \text{row}\{T_{N+1,m} P_m\} \\ \hat{J}_e &= \text{row}\{T_{N+1,m+1} S_{m+1,m}\} \end{aligned} \quad (5)$$

where $n, m = 1, \dots, N$ and the composite interbody transformation matrices are given by

$$T_{nm} = \begin{cases} T_{n,n-1} T_{n-1,n-2} \dots T_{m+1,m}, & m < n \\ \mathbf{1}, & m = n \\ \mathbf{0}, & m > n \end{cases}$$

The relationships implied by Eqs. (3) and (4) can be collected into the global form

$$\begin{bmatrix} v_0 \\ v_\ell \\ v_t \\ \dot{q}_e \end{bmatrix} = \begin{bmatrix} P_0 & \mathbf{0} & \mathbf{0} \\ \hat{T}_0 & \hat{T}_\theta & \hat{T}_e \\ \hat{J}_0 & \hat{J}_\theta & \hat{J}_e \\ \mathbf{0} & \mathbf{0} & \mathbf{1} \end{bmatrix} \begin{bmatrix} \dot{\rho}_0 \\ \dot{\theta} \\ \dot{q}_e \end{bmatrix} \Rightarrow v = \Upsilon(q) \dot{q} \quad (6)$$

which collects the kinematical constraints into one succinct equation. The definitions of v and Υ are obvious, and q was defined in Eq. (2).

It is now possible to isolate the differential kinematics describing the end-effector motion with respect to B_0 . From the third row of Eq. (6), we have

$$v_t = \hat{J}_0 \dot{\rho}_0 + v_{t0}, \quad v_{t0} \triangleq \hat{J}_\theta \dot{\theta} + \hat{J}_e \dot{q}_e \quad (7)$$

where v_{t0} is the relative payload velocity with respect to \mathcal{F}_0 . For control purposes, integrable coordinates are of greater interest; define ρ_t by

$$\dot{\rho}_t \triangleq P_t^{-1}(\rho_t) v_{t0}, \quad P_t = \text{diag}\{C_{N+1,0}, E_{N+1,0}\} \quad (8)$$

Hence, ρ_t is a 6×1 vector consisting of the payload position with respect to \mathcal{F}_0 (expressed in \mathcal{F}_0) and three Euler angles parameterizing the rotation matrix $C_{N+1,0}$. Combining Eqs. (7) and (8) gives the relationship

$$\begin{aligned} \dot{\rho}_t &= J_\theta(\theta, q_e) \dot{\theta} + J_e(\theta, q_e) \dot{q}_e, & J_\theta &\triangleq P_t^{-1} \hat{J}_\theta \\ & & J_e &\triangleq P_t^{-1} \hat{J}_e \end{aligned} \quad (9)$$

where J_θ shall be referred to as the rigid Jacobian and J_e as the elastic Jacobian. If the elastic dependence in the rigid Jacobian is suppressed, $J_\theta(\theta, \mathbf{0})$ can be identified with the Jacobian of the corresponding terrestrial-based, rigid manipulator.

Modified Output

The fundamental output variables are taken to be the spacecraft rates $\dot{\rho}_0$ and the corresponding variables for the end effector $\dot{\rho}_t$. We wish to generalize the latter quantities by separating the contributions of the joint motion from those due to the link deformations:

$$\dot{\rho}_{t\mu} \triangleq J_\theta \dot{\theta} + \mu J_e \dot{q}_e = \mu \dot{\rho}_t + (1 - \mu) J_\theta(\theta, q_e) \dot{\theta} \quad (10)$$

where μ is a real parameter. The true tip rates (with respect to B_0) are captured by $\mu = 1$ whereas $\mu = 0$ considers only joint-induced motion. For $\mu = -1$, the variables $\rho_{t\mu}$ shall be called the reflected

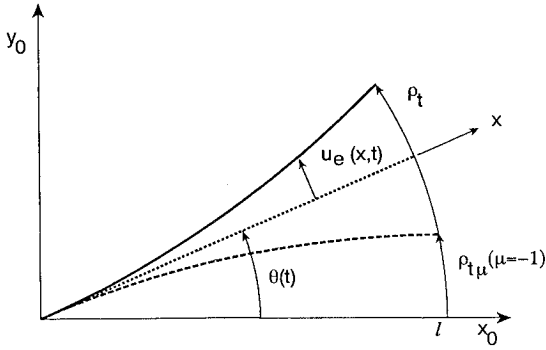


Fig. 2 A single flexible link.

tip position as suggested by Wang and Vidyasagar¹⁰ in the case of a single pinned-free planar beam. The latter situation is illustrated in Fig. 2 and Eq. (10) is the logical extension of this concept to multi-DOF arms.

It would be desirable if $\hat{\rho}_{t\mu}$ and $\rho_{t\mu}$ could be constructed from joint measurements $\{\theta, \dot{\theta}\}$ and tip measurements $\{\rho_t, \dot{\rho}_t\}$, thus excusing the requirement for direct measurements of the elastic coordinates q_e . In general, this is not possible unless J_θ is approximated by its rigid counterpart $J_\theta(\theta, \mathbf{0})$. In this case, $\rho_{t\mu}(t)$ can be fashioned from the tip position ρ_t (measured with respect to \mathcal{B}_0) and the rigid forward kinematics map. The total output vector consists of the spacecraft rates and the modified tip rates,

$$y_\mu \triangleq \begin{bmatrix} \dot{\rho}_0 \\ \dot{\rho}_{t\mu} \end{bmatrix} \quad (11)$$

and a corresponding modified input will be described in the next section.

Dynamics

The kinetic energy of the chain can be written as

$$T = \frac{1}{2} \begin{bmatrix} v_0^T & v_\ell^T & v_t^T & \dot{q}_e^T \end{bmatrix} \begin{bmatrix} M_{0,rr} & \mathbf{0} & \mathbf{0} & \mathbf{0} \\ \mathbf{0} & \hat{M}_{rr} & \mathbf{0} & \hat{M}_{re} \\ \mathbf{0} & \mathbf{0} & M_t & \mathbf{0} \\ \mathbf{0} & \hat{M}_{re}^T & \mathbf{0} & \hat{M}_{ee} \end{bmatrix} \begin{bmatrix} v_0 \\ v_\ell \\ v_t \\ \dot{q}_e \end{bmatrix} \quad (12)$$

$$\equiv \frac{1}{2} \dot{v}^T \hat{M} \dot{v}$$

where the matrices \hat{M}_{rr} , \hat{M}_{re} , and \hat{M}_{ee} are block diagonal assemblies of the corresponding body matrices defined subsequently. The rigid mass matrix is defined by

$$\hat{M}_{n,rr} \triangleq \begin{bmatrix} m_n & -c_n^x \\ c_n^x & \tilde{J}_n \end{bmatrix}, \quad M_t \triangleq \hat{M}_{N+1,rr} \quad (13)$$

where m_n , c_n , and \tilde{J}_n are the zeroth (mass), first, and second moments of inertia, respectively. For an exact treatment, the latter two are defined allowing for elastic deformation.¹⁵ The portion of the link mass matrices coupling rigid and elastic motions $\hat{M}_{n,re}$ is formed from the elastic momentum and (deformed) angular momentum coefficients.^{13,15}

The strain energy is given by

$$V(t) = \frac{1}{2} q^T \hat{K}(q) q, \quad \hat{K} \triangleq \text{diag}\{\mathbf{0}, \mathbf{0}, \hat{K}_{ee}(q_e)\} \quad (14)$$

$$\hat{K}_{ee} \triangleq \text{diag}\{\hat{K}_{n,ee}\}$$

$\hat{M}_{n,ee}$ and $\hat{K}_{n,ee}$ are the mass and strain energy matrices relative to the chosen basis functions. Geometric stiffening can be captured through the use of nonlinear strain displacement relations¹⁵ which leads to a quartic dependence on q_e in V and, hence, $\hat{K}_{n,ee}(q_{n,e})$ is a function of the elastic coordinates. In later numerical work, the selected basis functions are the constrained natural modes of each body and, hence, $\hat{M}_{n,ee} \equiv \mathbf{1}$ and $\hat{K}_{n,ee}(\mathbf{0})$ is a diagonal matrix of squared constrained natural frequencies.

Now, using Eq. (6), the kinetic energy given by Eq. (12) becomes

$$T = \frac{1}{2} \dot{q}^T M(q) \dot{q}, \quad M \triangleq \Upsilon^T(q) \hat{M} \Upsilon(q) = \begin{bmatrix} M_{00} & M_{0\theta} & M_{0e} \\ M_{0\theta}^T & M_{\theta\theta} & M_{\theta e} \\ M_{0e}^T & M_{\theta e}^T & M_{ee} \end{bmatrix} \quad (15)$$

where the global mass matrix M has been partitioned to agree with the definition of q in Eq. (2) and

$$M_{00} = \underline{P_0^T M_{0,rr} P_0} + \underline{\hat{T}_0^T \hat{M}_{rr} \hat{T}_0} + \underline{\hat{J}_0^T M_t \hat{J}_0} \quad (16)$$

$$M_{0\theta} = \underline{\hat{T}_0^T \hat{M}_{rr} \hat{T}_\theta} + \underline{\hat{J}_0^T M_t \hat{J}_\theta} \quad (17)$$

$$M_{0e} = \underline{\hat{T}_0^T \hat{M}_{rr} \hat{T}_e} + \underline{\hat{T}_0^T \hat{M}_{re}} + \underline{\hat{J}_0^T M_t \hat{J}_e} \quad (18)$$

$$M_{\theta\theta} = \underline{\hat{T}_\theta^T \hat{M}_{rr} \hat{T}_\theta} + \underline{\hat{J}_\theta^T M_t \hat{J}_\theta} \quad (19)$$

$$M_{\theta e} = \underline{\hat{T}_\theta^T \hat{M}_{rr} \hat{T}_e} + \underline{\hat{T}_\theta^T \hat{M}_{re}} + \underline{\hat{J}_\theta^T M_t \hat{J}_e} \quad (20)$$

$$M_{ee} = \underline{\hat{T}_e^T \hat{M}_{rr} \hat{T}_e} + \underline{\hat{T}_e^T \hat{M}_{re}} + \underline{\hat{M}_{re}^T \hat{T}_e} + \underline{\hat{J}_e^T M_t \hat{J}_e} + \underline{\hat{M}_{ee}} \quad (21)$$

Terms involving the payload and spacecraft have been underlined for future reference. The matrix M is symmetric and positive definite, and the matrix \hat{K} is symmetric and positive semidefinite.

To complete this section, it is assumed that \mathcal{B}_0 is fully actuated in translation and rotation. The column of forces/torques acting on it is denoted by $f_{0,c}$. The joint torques acting at the inboard end of each link will be designated $\tau_n(t)$ and $\tau \triangleq \text{col}\{\tau_n\}$. Hence, the virtual work of the nonconservative control influences is given by

$$\delta W_e = f_{0,c}^T P_0 \delta \rho_0 + \tau^T \delta \theta = \underline{\hat{f}_0^T} \delta \rho_0 + \tau^T \delta \theta \equiv f_c^T \delta q \quad (22)$$

where $\hat{f}_0 = P_0^T f_{0,c}$ is a column of forces and Euler torques and $f_c \triangleq \text{col}\{\hat{f}_0, \tau, \mathbf{0}\}$.

Equations of Motion

The equations of motion can be derived by forming the Lagrangian $L \triangleq T - V$. Hamilton's (extended) principle gives

$$\frac{d}{dt} \left(\frac{\partial L}{\partial \dot{q}} \right) - \frac{\partial L}{\partial q} = f_c$$

Applying these to the energy and work expressions (14), (15), and (22) yields

$$M(q) \ddot{q} + K(q) q = f_c(t) + f_{\text{non}}(q, \dot{q}) \quad (23)$$

where f_{non} are nonlinear terms which are quadratic in \dot{q} . An explicit description of f_{non} will not be needed. The stiffness term is constructed so that $Kq = \partial V / \partial q$ and, therefore, $K = \text{diag}\{\mathbf{0}, \mathbf{0}, K_{ee}\}$. If linear strain-displacement relations are used, $K_{ee} \equiv \hat{K}_{ee}$.

III. Linear Passivity Analysis

We now consider small motions in the vicinity of the constant configuration $q_d = \text{col}\{\rho_d, \theta_d, \mathbf{0}\}$. By abuse of notation, the variables $q(t)$ (and, therefore, ρ_0 , θ , and $\rho_{t\mu}$) will refer to motions relative to the set point. The linearized motion equations are given by

$$M(q_d) \ddot{q} + K(q_d) q = f_c(t) \quad (24)$$

Similarly, the linearized form of Eq. (10) becomes

$$\rho_{t\mu} = J_\theta(\theta_d, \mathbf{0}) \theta + \mu J_e(\theta_d, \mathbf{0}) q_e \quad (25)$$

For the duration of this section the set-point dependence of $M(q_d)$, $K(q_d)$, $J_\theta(\theta_d, \mathbf{0})$, and $J_e(\theta_d, \mathbf{0})$ will not be displayed.

Consider the eigenvalue problem corresponding to the homogeneous form of Eq. (24):

$$-\omega_\alpha^2 M q_\alpha + K q_\alpha = \mathbf{0} \quad (26)$$

where ω_α are the vibration frequencies. The rigid modes ($\omega_\alpha \equiv 0$) span the null space of \mathbf{K} ,

$$\mathbf{K}\mathbf{Q}_r = \mathbf{0}, \quad \mathbf{Q}_r = \begin{bmatrix} \mathbf{1} & \mathbf{0} \\ \mathbf{0} & \mathbf{1} \\ \mathbf{0} & \mathbf{0} \end{bmatrix}$$

The first column corresponds to the six rigid modes of \mathcal{B}_0 , whereas the second corresponds to the rigid rotational motions of each joint. For the vibrational modes, partition the eigenvector according to Eq. (2): $\mathbf{q}_\alpha = \text{col}\{\rho_{0\alpha}, \theta_\alpha, \mathbf{q}_{e\alpha}\}$. They satisfy the standard orthonormality relations

$$\mathbf{q}_\alpha^T \mathbf{M} \mathbf{q}_\beta = \delta_{\alpha\beta}, \quad \mathbf{q}_\alpha^T \mathbf{K} \mathbf{q}_\beta = \omega_\alpha^2 \delta_{\alpha\beta}$$

and the \mathbf{q}_α are also orthogonal to \mathbf{Q}_r (with respect to \mathbf{M} and \mathbf{K}). These modes have been termed hinges-free vehicle modes by Hablani,¹⁶ but we shall call them unconstrained modes (\mathcal{B}_0 free, joints unlocked). They represent the natural extension of the pinned-free modes of a single link.

The eigenvectors form a complete set. Hence, the solution to the linearized motion equation can be expanded as follows:

$$\rho_0(t) = \rho_r(t) + \sum_{\alpha=1}^{N_e} \eta_\alpha(t) \rho_{0\alpha}$$

$$\theta(t) = \theta_r(t) + \sum_{\alpha=1}^{N_e} \eta_\alpha(t) \theta_\alpha, \quad N_e = s_1 + \dots + s_N \quad (27)$$

$$\mathbf{q}_e(t) = \sum_{\alpha=1}^{N_e} \eta_\alpha(t) \mathbf{q}_{e\alpha}$$

where $\{\rho_r, \theta_r\}$ are the rigid modal coordinates and η_α is associated with \mathbf{q}_α . Substituting this modal expansion into Eq. (24) and observing the orthonormality relationships gives

$$\underbrace{\begin{bmatrix} \mathbf{M}_{00} & \mathbf{M}_{0\theta} \\ \mathbf{M}_{\theta 0}^T & \mathbf{M}_{\theta\theta} \end{bmatrix}}_{\tilde{\mathbf{M}}} \begin{bmatrix} \ddot{\rho}_r \\ \ddot{\theta}_r \end{bmatrix} = \begin{bmatrix} \hat{\mathbf{f}}_0 \\ \boldsymbol{\tau} \end{bmatrix} \quad (28)$$

$$\ddot{\eta}_\alpha + \omega_\alpha^2 \eta_\alpha = \rho_{0\alpha}^T \hat{\mathbf{f}}_0 + \theta_\alpha^T \boldsymbol{\tau}, \quad \alpha = 1, \dots, N_e$$

The mass matrix $\tilde{\mathbf{M}}$ is that corresponding to the system if it were rigid. The partition $\mathbf{M}_{0\theta}$ fully described in Eq. (17) captures the coupling between the rigid joint motion and the spacecraft motion. It is at this point that structural damping, neglected so far, could be most easily incorporated in the form of modal damping factors. Since light damping would not substantially change the subsequent results, it will be neglected.

Assumption 1

The manipulator is nonredundant ($N = 6$), and the reference configuration \mathbf{q}_d is kinematically nonsingular,

$$\text{rank } \mathbf{J}_\theta = 6 \quad (29)$$

This ensures that all possible local joint motions produce payload motion. The following modified version of the joint torques can then be defined:

$$\hat{\boldsymbol{\tau}}(t) \triangleq \mathbf{J}_\theta^{-T} \boldsymbol{\tau}(t) \quad (30)$$

The assumption $N = 6$ is required for invertibility of \mathbf{J}_θ . For $N > 6$, \mathbf{J}_θ^{-1} can be replaced with the pseudoinverse but this complicates the subsequent discussion. For rigid robots, it is well known that $\hat{\boldsymbol{\tau}}$ is the equivalent set of (generalized) forces applied at the end effector. They can be combined with the spacecraft inputs by defining

$$\mathbf{u}(t) \triangleq \text{col}\{\hat{\mathbf{f}}_0, \hat{\boldsymbol{\tau}}\} \quad (31)$$

to produce an input vector with the same dimension as \mathbf{y}_μ , i.e., 12. In the following, Laplace transformed quantities will be indicated by the argument s .

Lemma 1

The transfer matrix relating the modified input $\mathbf{u}(s)$ to the modified output $\mathbf{y}_\mu(s)$ is given by

$$\mathbf{G}_\mu(s) = \frac{1}{s} \begin{bmatrix} \mathbf{I} & \mathbf{0} \\ \mathbf{0} & \mathbf{J}_\theta \end{bmatrix} \tilde{\mathbf{M}}^{-1} \begin{bmatrix} \mathbf{I} & \mathbf{0} \\ \mathbf{0} & \mathbf{J}_\theta^T \end{bmatrix} + \sum_{\alpha=1}^{N_e} \frac{s}{s^2 + \omega_\alpha^2} \mathbf{C}_\alpha \mathbf{B}_\alpha^T \quad (32)$$

where

$$\mathbf{C}_\alpha \triangleq \begin{bmatrix} \rho_{0\alpha} \\ \mathbf{J}_\theta \theta_\alpha + \mu \mathbf{J}_e \mathbf{q}_{e\alpha} \end{bmatrix}, \quad \mathbf{B}_\alpha^T \triangleq [\rho_{0\alpha}^T \quad \theta_\alpha^T \mathbf{J}_\theta^T] \quad (33)$$

Proof

Taking Laplace transforms of the output defined by Eqs. (11) and (25) and noting the modal expansions (27) gives

$$\mathbf{y}_\mu(s) = s \begin{bmatrix} \rho_r(s) \\ \mathbf{J}_\theta \theta_r(s) \end{bmatrix} + s \sum_{\alpha=1}^{N_e} \begin{bmatrix} \rho_{0\alpha} \\ \mathbf{J}_\theta \theta_\alpha + \mu \mathbf{J}_e \mathbf{q}_{e\alpha} \end{bmatrix} \eta_\alpha(s) \quad (34)$$

Laplace transforming the modal equations (28) and substituting into Eq. (34) while observing the definition of \mathbf{u} in Eq. (31) gives $\mathbf{y}_\mu(s) = \mathbf{G}_\mu(s) \mathbf{u}(s)$ where \mathbf{G}_μ is given in the statement of the Lemma. \square

Definition 1

A square matrix function $\mathbf{G}(s)$ is positive real¹⁷ if 1) All elements $\mathbf{G}(s)$ are analytic for $\text{Re}\{s\} > 0$, 2) $\mathbf{G}(s)$ is real for real positive s , and 3) $\mathbf{G}(s) + \mathbf{G}^H(s) \geq 0$ for $\text{Re}\{s\} > 0$. The main importance of positive real functions is that they can be stabilized by any feedback compensator $\mathbf{H}(s)$ which is strictly positive real, i.e., $\mathbf{H}(s - \epsilon)$ is PR for some $\epsilon > 0$, and the region of analyticity in 1 is extended to include the imaginary axis.

Using a result of Anderson and Vongpanitlerd,¹⁷ $\mathbf{G}_\mu(s)$ is positive real if the coefficient matrices of the scalar positive real functions $1/s$ and $s/(s^2 + \omega_\alpha^2)$ are symmetric and at least positive semidefinite. This is certainly the case when $\mu \equiv 0$ which corresponds to considering only the joint-induced tip rate. In the present situation, the transfer matrix would be lossless¹⁷ reflecting conservation of energy in the unforced system. Before tackling the case of nonzero μ , we shall connect our results with those of Pota and Vidyasagar.¹¹

Begin by eliminating the spacecraft degrees of freedom in Eqs. (32) and (33):

$$s \rho_{t\mu}(s) = \left[\frac{1}{s} \mathbf{J}_\theta \mathbf{M}_{\theta\theta}^{-1} \mathbf{J}_\theta^T + \sum_{\alpha=1}^{N_e} \frac{s}{s^2 + \omega_\alpha^2} (\mathbf{J}_\theta \theta_\alpha + \mu \mathbf{J}_e \mathbf{q}_{e\alpha}) (\mathbf{J}_\theta \theta_\alpha)^T \right] \hat{\boldsymbol{\tau}}(s) \quad (35)$$

We see that in the case of a terrestrial-based flexible manipulator, the requirement for positive realness is positive semidefiniteness of $(\mathbf{J}_\theta \theta_\alpha + \mu \mathbf{J}_e \mathbf{q}_{e\alpha}) (\mathbf{J}_\theta \theta_\alpha)^T$ for each vibration mode. Further specializing to the case of a single link, consider the scalar form of Eq. (35) where $\rho_{t\mu}$ was illustrated in Figure 2 and $\mathbf{M}_{\theta\theta}$ becomes the link moment of inertia about the joint axis. The PR condition for each mode becomes

$$(\mathbf{J}_\theta \theta_\alpha)^2 + \mu (\mathbf{J}_e \mathbf{q}_{e\alpha}) (\mathbf{J}_\theta \theta_\alpha) \geq 0 \quad (36)$$

The tip position of the link can be written as

$$\rho_r(t) = \ell \theta(t) + u_e(\ell, t), \quad u_e(x, t) = \sum_{\beta=1}^{s_1} \psi_{1\beta}(x) q_{1\beta}(t)$$

and comparing with Eq. (9), we can identify the Jacobian matrices as $\mathbf{J}_\theta = \ell$, $\mathbf{J}_e = \text{row}\{\psi_{1\beta}(\ell)\}$. From the eigenvectors $\mathbf{q}_\alpha = \text{col}\{\theta_\alpha, \mathbf{q}_{e\alpha}\}$, the pinned-free modes of the beam can be constructed as

$$\rho_{\alpha}(x) = x \theta_\alpha + u_{e\alpha}(x), \quad u_{e\alpha}(x) = \sum_{\beta} \psi_{1\beta}(x) q_{e\alpha,\beta}$$

where the identifications $\theta_\alpha = \rho'_\alpha(0)$ and $u_{e\alpha}(\ell) = \mathbf{J}_e \mathbf{q}_{e\alpha} = \rho_\alpha(\ell) - \ell \rho'_\alpha(0)$ can be made. The requirement for positive realness, Eq. (36), then simplifies to

$$(1 - \mu)\ell \rho'_\alpha(0)^2 + \mu \rho'_\alpha(0) \rho_\alpha(\ell) \geq 0$$

This inequality has been shown to hold for each α for the pinned-free modes of a uniform beam when $\mu = -1$ (Ref. 11). An analytical representation for $\rho_\alpha(x)$ was used. Therefore, the mapping between joint torque and reflected tip rate is positive real. Although Eq. (36) clearly holds for $\mu = 0$, in general it does not hold when $\mu = 1$ for a beam without payload or hub inertia.

Let us now enumerate possible extensions of this result. For the terrestrial-based multilink flexible manipulator, it does not seem possible that the transfer function in Eq. (35) can be PR in general. A sufficient requirement is that there exist constants κ_α such that $\mathbf{J}_e \mathbf{q}_{e\alpha} = \kappa_\alpha \mathbf{J}_\theta \theta_\alpha$ and $1 + \mu \kappa_\alpha \geq 0$. Despite the single-link success, this is not expected to hold in general. However, there is one case of practical interest where not only does it hold but in the spacecraft-based case, the matrix products $\mathbf{C}_\alpha \mathbf{B}_\alpha^T$ defined by Eq. (33) are also positive semidefinite.

Assumption 2

The spacecraft and payload are much more massive than the individual links, i.e.,

$$\mathbf{M}_{0,rr} \gg \hat{\mathbf{M}}_{n,rr}, \quad \mathbf{M}_i \gg \hat{\mathbf{M}}_{n,rr}, \quad n = 1, \dots, N \quad (37)$$

where the ordering is the usual one for symmetric positive-definite matrices.

One need only consider the common situation of Shuttle RMS satellite deployment to realize that the proposed scenario is not unduly restrictive. For this situation we have the following theorem.

Theorem 1 (Main Result)

When assumptions 1 and 2 hold, the vibration modes satisfy

$$\rho_{0\alpha} \doteq \mathbf{0}, \quad \mathbf{J}_\theta \theta_\alpha + \mathbf{J}_e \mathbf{q}_{e\alpha} \doteq \mathbf{0}, \quad \alpha = 1, \dots, N_e \quad (38)$$

(The symbol \doteq will be used for those equalities that hold by virtue of assumptions 1 and 2). In this case, the transfer matrix $\mathbf{G}_\mu(s)$ is positive real for $\mu \leq 1$.

Proof

The structure of \mathbf{M} in Eq. (15) and $\mathbf{K} \equiv \hat{\mathbf{K}}(q_d)$ in Eq. (14) gives the following for the first two rows contained in the eigenequation (26):

$$\mathbf{M}_{00} \rho_{0\alpha} + \mathbf{M}_{0\theta} \theta_\alpha + \mathbf{M}_{0e} \mathbf{q}_{e\alpha} = \mathbf{0}$$

$$\mathbf{M}_{0\theta}^T \rho_{0\alpha} + \mathbf{M}_{\theta\theta} \theta_\alpha + \mathbf{M}_{\theta e} \mathbf{q}_{e\alpha} = \mathbf{0}$$

Assumptions 1 and 2 allow us to use only the underlined terms in Eqs. (16–20). Performing these substitutions gives

$$\mathbf{P}_0^T \mathbf{M}_{0,rr} \mathbf{P}_0 \rho_{0\alpha} + \hat{\mathbf{J}}_0^T \mathbf{M}_i [\hat{\mathbf{J}}_0 \rho_{0\alpha} + \hat{\mathbf{J}}_\theta \theta_\alpha + \hat{\mathbf{J}}_e \mathbf{q}_{e\alpha}] \doteq \mathbf{0}$$

$$\hat{\mathbf{J}}_\theta^T \mathbf{M}_i [\hat{\mathbf{J}}_0 \rho_{0\alpha} + \hat{\mathbf{J}}_\theta \theta_\alpha + \hat{\mathbf{J}}_e \mathbf{q}_{e\alpha}] \doteq \mathbf{0}$$

Given assumption 1 and the positive definiteness of \mathbf{M}_i and $\mathbf{M}_{0,rr}$, we conclude that

$$\rho_{0\alpha} \doteq \mathbf{0}, \quad \hat{\mathbf{J}}_\theta \theta_\alpha + \hat{\mathbf{J}}_e \mathbf{q}_{e\alpha} \doteq \mathbf{0}, \quad \alpha = 1, \dots, N_e \quad (39)$$

Premultiplying the second relationship by \mathbf{P}_i^{-1} and noting Eq. (9) establishes the second-half of Eq. (38). Therefore, the coefficient matrix in the α th term of \mathbf{G}_μ takes the form

$$\mathbf{C}_\alpha \mathbf{B}_\alpha^T \doteq \begin{bmatrix} \mathbf{0} & \mathbf{0} \\ \mathbf{0} & (1 - \mu) \mathbf{J}_\theta \theta_\alpha \theta_\alpha^T \mathbf{J}_\theta^T \end{bmatrix} \quad (40)$$

which is positive semidefinite provided $\mu \leq 1$. Hence, $\mathbf{G}_\mu(s)$ is PR. \square

Theorem 1 shows that the velocity produced at the end effector from joint motion in mode α is equal and opposite to that created by the link deformations. Hence, in this limiting situation neither the spacecraft nor the payload participate in the vibration mode. The vibrations are internalized among the joints and link deformations, and the modes may be described as clamped-clamped. Interestingly, the properties (38) are due to the spacecraft and payload mass properties which provide boundary conditions, yet the vibration frequencies will asymptotically depend only on the link properties. From Eq. (40), positive realness can be obtained when $\mu = 1$, i.e., using the true tip rates. In this case, the transfer matrix \mathbf{G}_μ behaves in a rigid fashion which would seem desirable. However, the vibration modes in a state-space realization would become unobservable via \mathbf{y}_μ since $\mathbf{C}_\alpha \doteq \mathbf{0}$. This situation is avoided when $\mu < 1$, and decreasing μ enhances the observability of the vibration modes.

The major application of Theorem 1 is to control system design. By the passivity theorem (precisely stated in Sec. IV), any strictly passive feedback compensator will stabilize the system. For example, we could take

$$\begin{bmatrix} \hat{\mathbf{f}}_0(s) \\ \hat{\boldsymbol{\tau}}(s) \end{bmatrix} = - \begin{bmatrix} \mathbf{H}_0(s) & \mathbf{0} \\ \mathbf{0} & \mathbf{H}_i(s) \end{bmatrix} \begin{bmatrix} s \rho_0(s) \\ s \rho_{i\mu}(s) \end{bmatrix} \quad (41)$$

where $\mathbf{H}_0(s)$ and $\mathbf{H}_i(s)$ are SPR and $\hat{\mathbf{f}}_{0,c}(s) = \mathbf{P}_0^{-T} \hat{\mathbf{f}}_{0,c}(s)$, $\boldsymbol{\tau}(s) = \mathbf{J}_\theta^T \hat{\boldsymbol{\tau}}(s)$. Hence, the stationkeeping and attitude control for \mathbf{B}_0 can proceed independently of that for positioning of the end effector. It has been noted¹⁸ that most control strategies that work in a terrestrial setting can also be employed for space-based rigid manipulators. This is borne out by the present result. A candidate controller for both is of the form $\mathbf{H}(s) = \mathbf{K}_d + \mathbf{K}_p s^{-1}$ with \mathbf{K}_d and \mathbf{K}_p positive definite which represents PD control. The robustness properties of this controller have been well studied for attitude control of flexible spacecraft.² The design of dynamic SPR compensators has received some attention^{3,19} and they have been applied to the control of flexible manipulators with joint feedback.²⁰

IV. Nonlinear Passivity Analysis

Since the positive real property of the linear transfer function holds for generic nonsingular configurations, it is worthwhile investigating the full nonlinear system. PR transfer functions are an example of the more general notion of passive systems.^{21–23} The following general definitions are taken from Ref. 22 where the reader will find a complete description of input-output stability and precise definitions of the function space \mathcal{L}_2 and its extended counterpart \mathcal{L}_{2e} . (By abuse of notation, we omit the subscripts indicating the length of the vector elements in \mathcal{L}_2 and \mathcal{L}_{2e} .) The norm in \mathcal{L}_2 will be indicated by $\|\cdot\|_2$.

Definition 2

A square system \mathbf{G} with input $\mathbf{u}(t) \in \mathcal{L}_{2e}$ and output $\mathbf{y}(t) = \mathbf{G}(\mathbf{u}) \in \mathcal{L}_{2e}$ is passive if

$$\int_0^T \mathbf{y}^T \mathbf{u} dt = \int_0^T \mathbf{u}^T \mathbf{G}(\mathbf{u}) dt \geq 0, \quad \forall \mathbf{u}(t) \in \mathcal{L}_{2e}, \quad \forall T > 0$$

Definition 3

The preceding system is strictly passive if there exists $\varepsilon > 0$ such that

$$\int_0^T \mathbf{u}^T \mathbf{G}(\mathbf{u}) dt \geq \varepsilon \int_0^T \mathbf{u}^T \mathbf{u} dt, \quad \forall \mathbf{u}(t) \in \mathcal{L}_{2e}, \quad \forall T > 0$$

It can be shown that for linear, time-invariant systems, positive realness is equivalent to passivity²³ and strict positive realness with positive-definite high-frequency gain implies strict passivity.²¹

Definition 4

The system \mathbf{G} is \mathcal{L}_2 -stable if $\mathbf{u} \in \mathcal{L}_2$ implies that $\mathbf{G}(\mathbf{u}) \in \mathcal{L}_2$. With reference to the feedback system in Fig. 3, there is the following powerful theorem.

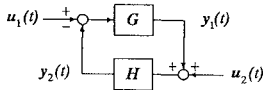


Fig. 3 Feedback system.

Passivity Theorem^{21–24}

If G is passive and H is strictly passive with finite gain (i.e., there exists γ , $0 < \gamma < \infty$, such that $\|H(\mathbf{u})\|_2 \leq \gamma \|\mathbf{u}\|_2$) then the feedback system depicted in Fig. 3 is \mathcal{L}_2 -stable in the sense that if $\{\mathbf{u}_1, \mathbf{u}_2\} \in \mathcal{L}_2$ then $\{\mathbf{y}_1, \mathbf{y}_2\} \in \mathcal{L}_2$. In this case, the errors $\mathbf{e}_1 \triangleq \mathbf{u}_1 - \mathbf{y}_2$ and $\mathbf{e}_2 \triangleq \mathbf{u}_2 + \mathbf{y}_1$ are also in \mathcal{L}_2 . If the finite gain assumption on H is not honored and if $\mathbf{u}_2 \equiv 0$, $\mathbf{u}_1 \in \mathcal{L}_2$ implies that $\mathbf{y}_1 \in \mathcal{L}_2$ but \mathbf{e}_1 is not necessarily square integrable.²¹

Although this is an input-output result, it has been extended to a nonlinear state-space setting.²⁵ Essentially, \mathcal{L}_2 -stability of the feedback system coupled with reachability and zero-state detectability of each system (controllability and observability for linear systems) implies global asymptotic stability of the origin for the unforced system ($\mathbf{u}_1 = \mathbf{u}_2 \equiv \mathbf{0}$).

We will now show that the mapping from $\mathbf{u}(t)$ to $\mathbf{y}_\mu(t)$ for the problem under consideration is passive for $\mu \leq 1$. For the system defined by Eq. (23), define the Hamiltonian by

$$H(t) = \dot{\mathbf{q}}^T \frac{\partial L}{\partial \dot{\mathbf{q}}} - L = \frac{1}{2} \dot{\mathbf{q}}^T \mathbf{M}(\mathbf{q}) \dot{\mathbf{q}} + \frac{1}{2} \mathbf{q}^T \hat{\mathbf{K}}(\mathbf{q}) \mathbf{q}$$

which is the total energy. Using Lagrange's equations, it follows that

$$\frac{dH}{dt} = \mathbf{f}_c^T \dot{\mathbf{q}} = \hat{\mathbf{f}}_0^T \dot{\rho}_0 + \tau^T \dot{\theta} = \hat{\mathbf{f}}_0^T \dot{\rho}_0 + \hat{\tau}^T \mathbf{J}_\theta \dot{\theta} \quad (42)$$

or, in words, the total energy evolves in accordance with the work done by the control influences. A nice demonstration of this result in the case of a rigid terrestrial-based manipulator is provided in Ref. 4.

Using definition 2, the passivity of the mapping from modified input to modified output depends on the integral

$$\begin{aligned} \int_0^T \mathbf{y}_\mu^T \mathbf{u} \, dt &= \int_0^T [\hat{\mathbf{f}}_0^T \dot{\rho}_0 + \hat{\tau}^T \mathbf{J}_\theta \dot{\theta} + \mu \hat{\tau}^T \mathbf{J}_e \dot{\mathbf{q}}_e] \, dt \\ &= H(T) - H(0) + \mu \int_0^T \tau^T \mathbf{J}_\theta^{-1} \mathbf{J}_e \dot{\mathbf{q}}_e \, dt \end{aligned} \quad (43)$$

where we have noted Eqs. (11) and (10) and used Eq. (42). Consistent with an input-output treatment, we take $H(0) = 0$, and it is immediately clear that the mapping is passive when $\mu = 0$ since $H(T) \geq 0$. It must be emphasized that this holds regardless of any approximations governing the spacecraft and payload and is a ramification of the effective collocation of actuation and sensing.

For nonzero μ , demonstration of passivity is made difficult by the last integral in Eq. (43). It can be simplified under the assumptions made by appealing to d'Alembert's form of the principle of virtual work. Given assumptions 1 and 2, the only generalized inertial forces that need be considered are those associated with the motion of \mathcal{B}_0 and \mathcal{B}_{N+1} . This is equivalent to including only the underlined terms in Eqs. (16–21) and permits a treatment of \mathbf{f}_{non} , which is consistent with this. The inertia forces are defined by

$$\begin{aligned} \mathbf{f}_0^{(i)} &= -\frac{d}{dt} (\mathbf{T}_{0I}^T \mathbf{M}_{0,rr} \mathbf{v}_0), & \mathbf{T}_{0I} &\triangleq \begin{bmatrix} \mathbf{C}_{0I} & -\mathbf{C}_{0I} \mathbf{r}_{I0}^\times \\ \mathbf{0} & \mathbf{C}_{0I} \end{bmatrix} \\ \mathbf{f}_i^{(i)} &= -\frac{d}{dt} (\mathbf{T}_{N+1,I}^T \mathbf{M}_i \mathbf{v}_i), & \mathbf{T}_{N+1,I} &\triangleq \begin{bmatrix} \mathbf{C}_{N+1,I} & -\mathbf{C}_{N+1,I} \mathbf{r}_{i,N+1}^\times \\ \mathbf{0} & \mathbf{C}_{N+1,I} \end{bmatrix} \end{aligned}$$

where some care has been taken to perform the differentiation in \mathcal{F}_I . The off-diagonal partitions in \mathbf{T}_{0I} and $\mathbf{T}_{N+1,I}$ capture the contribution of the momentum to the total angular momentum with respect to the origin of \mathcal{F}_I .

The virtual work of the elastic forces must equal that of the applied and inertial forces.

$$\begin{aligned} \delta \mathbf{q}_e^T \mathbf{K}_{ee} \mathbf{q}_e &\doteq \mathbf{f}_{0,c}^T \mathbf{P}_0 \delta \rho_0 + \tau^T \delta \theta + (\mathbf{T}_{I0}^T \mathbf{f}_0^{(i)})^T \mathbf{P}_0 \delta \rho_0 \\ &+ (\mathbf{T}_{i,N+1}^T \mathbf{f}_i^{(i)})^T (\hat{\mathbf{J}}_0 \delta \rho_0 + \hat{\mathbf{J}}_\theta \delta \theta + \hat{\mathbf{J}}_e \delta \mathbf{q}_e) \end{aligned} \quad (44)$$

where the definitions of \mathbf{v}_0 , Eq. (4), and \mathbf{v}_i , Eq. (7), have been used to construct the Cartesian virtual displacements. The transformation matrices introduced in Eq. (44), satisfy $\mathbf{T}_{I0} \equiv \mathbf{T}_{0I}^{-1}$ and $\mathbf{T}_{i,N+1} \equiv \mathbf{T}_{N+1,I}^{-1}$. They are used to correctly form the inertial force and torque in \mathcal{F}_0 and \mathcal{F}_{N+1} , respectively.

Since $\delta \rho_0$, $\delta \theta$, and $\delta \mathbf{q}_e$ are arbitrary, we conclude from Eq. (44) that

$$-\hat{\mathbf{J}}_0^T \mathbf{T}_{I,N+1}^T \mathbf{f}_i^{(i)} - \mathbf{P}_0^T \mathbf{T}_{I0}^T \mathbf{f}_0^{(i)} \doteq \hat{\mathbf{f}}_0 \quad (45)$$

$$-\hat{\mathbf{J}}_\theta^T \mathbf{T}_{i,N+1}^T \mathbf{f}_i^{(i)} \doteq \tau \quad (46)$$

$$-\hat{\mathbf{J}}_e^T \mathbf{T}_{i,N+1}^T \mathbf{f}_i^{(i)} + \mathbf{K}_{ee} \mathbf{q}_e \doteq \mathbf{0} \quad (47)$$

which is a restatement of the motion equations (23) under assumptions 1 and 2. If $\mathbf{f}_0^{(i)}$ and $\mathbf{f}_i^{(i)}$ are replaced by static applied forces at the base and tip, respectively, then the above are the requirements for static equilibrium. This gives a dual interpretation for the elastic Jacobian \mathbf{J}_e ; it enables the static deflections produced by tip loads to be calculated using Eq. (47). Combining Eqs. (46) and (47) gives

$$\mathbf{K}_{ee} \mathbf{q}_e(t) \doteq -\hat{\mathbf{J}}_e^T \hat{\mathbf{J}}_\theta^{-T} \tau = -\mathbf{J}_e^T \mathbf{J}_\theta^{-T} \tau(t) \quad (48)$$

which must hold for payload/spacecraft-dominated dynamics. Equation (48) illustrates a static relationship between applied torque and elastic deformation. This approximate relation should be very useful for trajectory planning since historically one of the challenges for flexible manipulators has been a specification for the elastic coordinates.

Premultiplication of Eq. (48) by $\dot{\mathbf{q}}_e^T$ yields

$$\dot{\mathbf{q}}_e^T \mathbf{K}_{ee} \mathbf{q}_e = \frac{dV}{dt} \doteq -\dot{\mathbf{q}}_e^T \mathbf{J}_e^T \mathbf{J}_\theta^{-T} \tau$$

which upon integration can be substituted into Eq. (43). Taking $H(0) = V(0) = 0$ gives the desired result, that is,

$$\int_0^T \mathbf{y}_\mu^T \mathbf{u} \, dt \doteq H(T) - \mu V(T) = T(T) + (1 - \mu)V(T) \quad (49)$$

which is clearly non-negative when $\mu \leq 1$. We conclude that under assumptions 1 and 2, the nonlinear scenario provides the same conclusion as the linear case (theorem 1). In particular, the mapping from modified spacecraft forces and joint torques to spacecraft rates and (partially) reflected tip rates is passive. By the passivity theorem, any strictly passive feedback compensator with finite gain will stabilize the system independent of the manipulator properties.

V. Numerical Example

The goal of the present section is to illustrate the key results given in Eqs. (38) and (48) in the context of a six-degree-of-freedom manipulator, modeled after the Space Shuttle remote manipulator (SRMS) arm. Included in the model is the Space Shuttle and a payload, modeled by a cylindrical drum to represent a spin-stabilized satellite. The properties of the members of the system are summarized in Table 1 and the architecture of the arm is shown in Fig. 4. The only flexible bodies are links 2 and 3 which are the lower- and upper-arm booms.

Each of the flexible booms is modeled using the natural constrained modes for discretization. The expansion for the elastic deflection in each boom is given by

$$\begin{aligned} \mathbf{u}_e(\mathbf{r}, t) &= \sum_{\alpha=1}^{s_u} \begin{bmatrix} u_\alpha \\ 0 \\ 0 \end{bmatrix} q_{u\alpha}(t) + \sum_{\alpha=1}^{s_v} \begin{bmatrix} -y v'_\alpha \\ v_\alpha \\ 0 \end{bmatrix} q_{v\alpha}(t) \\ &+ \sum_{\alpha=1}^{s_w} \begin{bmatrix} -z w'_\alpha \\ 0 \\ w_\alpha \end{bmatrix} q_{w\alpha}(t) + \sum_{\alpha=1}^{s_f} \begin{bmatrix} 0 \\ -z \phi_\alpha \\ \gamma \phi_\alpha \end{bmatrix} q_{f\alpha}(t) \end{aligned}$$

Table 1 Properties of the SRMS

Property	ℓ , m	Mass, kg	J_n^r , kg·m ²	J_n^p , kg·m ²	J_n^y , kg·m ²
Space Shuttle (r_{01}) ^a		93,270	1.17×10^6	9.1×10^6	9.5×10^6
Link 1	0.9	95	0.2	25.75	25.75
Link 2	6.4	138	0.4	1884.36	1884.36
Link 3	7.0	85	0.4	1388.53	1388.53
Link 4	0.5	8	0.2	0.76	0.76
Link 5	0.8	44	0.2	9.49	9.49
Link 6	0.6	41	0.2	5.02	5.02
Payload	–	15,000	30,000	515,000	515,000
Elastic stiffnesses		EI , N·m ²	GJ , N·m ²		EA , N
Link 2		4.046×10^6	2.040×10^6		2.790×10^9
Link 3		2.812×10^6	1.417×10^6		1.194×10^9

$${}^a(r_{01} = [-10.88 \ -2.45 \ 0.93]^T \text{ m}).$$

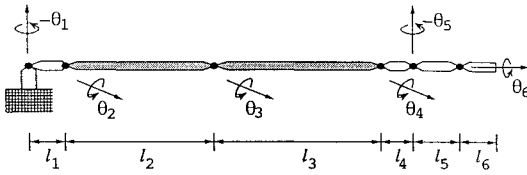


Fig. 4 Architecture of the SRMS.

where $v_\alpha(x) = w_\alpha(x)$ are the normalized bending mode shapes of a cantilevered uniform Euler–Bernoulli beam, and the functions $u_\alpha(x)$ and $\phi_\alpha(x)$ are the normalized stretching and torsional mode shapes of a uniform rod. Each boom is modeled with six modes: two bending modes in each of the in-plane and out-of-plane directions, one stretch mode, and one torsional mode.

Once the basis functions have been specified, the mass and stiffness matrices for the links and the various integrals of the basis functions required for evaluation of the motion equations can be derived. All modal integrals required have been performed analytically for the present choice of shape functions. The elastic mass matrices and the (nominal) stiffness matrices have the simple diagonal forms $\hat{M}_{n,ee} = \text{diag}\{1\}$, $\hat{K}_{n,ee}(\mathbf{0}) = \text{diag}\{\omega_{n\alpha}^2\}$ where $\omega_{n\alpha}$ are the natural frequencies of the body in isolation and cantilevered at the inboard articulation point. The 3-2-1 Euler sequences are used to describe both the spacecraft and payload orientations. The matrix \mathbf{M} is assembled according to Eqs. (15), (12), (6), and (5), and the matrix Υ is evaluated at $\mathbf{q}_d = \text{col}\{\mathbf{0}, \boldsymbol{\theta}_d, \mathbf{0}\}$ where $\boldsymbol{\theta}_d$ is as follows:

$$\begin{aligned} \theta_{d1} &= \pi/6, & \theta_{d2} &= \pi/2, & \theta_{d3} &= -\pi/4 \\ \theta_{d4} &= -\pi/4, & \theta_{d5} &= \pi/6, & \theta_{d6} &= 0 \end{aligned}$$

The datum for each joint angle is as given in Fig. 4 and because of space limitations only this configuration is treated.

We wish to numerically examine the size of the spacecraft modal coefficients $\rho_{0\alpha}$ and the tip modal coefficients $\mathbf{J}_\theta \boldsymbol{\theta}_\alpha + \mathbf{J}_e \mathbf{q}_{e\alpha}$. Given the mixed translational/rotational character of these six-dimensional quantities, let us define the following norms: if $\mathbf{x}^T = [x_1 \ x_2 \ \dots \ x_6]$ then

$$\|\mathbf{x}\|_t \triangleq [x_1^2 + x_2^2 + x_3^2]^{1/2}, \quad \|\mathbf{x}\|_b \triangleq [x_4^2 + x_5^2 + x_6^2]^{1/2}$$

For each vibration mode, the following quantities are proposed as appropriate norms:

$$E_{t\rho,\alpha} = \frac{\|\rho_{0\alpha}\|_t}{\|\mathbf{J}_\theta \boldsymbol{\theta}_\alpha\|_t}, \quad E_{t\theta,\alpha} = \frac{\|\mathbf{J}_\theta \boldsymbol{\theta}_\alpha + \mathbf{J}_e \mathbf{q}_{e\alpha}\|_t}{\|\mathbf{J}_\theta \boldsymbol{\theta}_\alpha\|_t}$$

and also the corresponding bottom quantities $E_{b\theta,\alpha}$ and $E_{b\rho,\alpha}$. The dependence of these quantities on the spacecraft and payload mass characteristics will now be illustrated. For the first situation, we replace the spacecraft mass matrix $\mathbf{M}_{0,rr}$ with $\varepsilon_0 \mathbf{M}_{0,rr}$ and vary ε_0

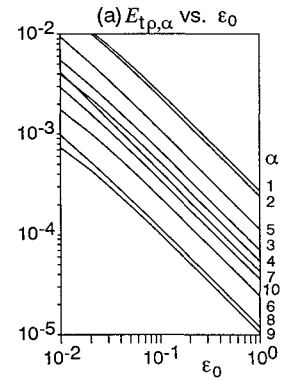


Fig. 5a Norms of the spacecraft modal coefficient vs. spacecraft size.

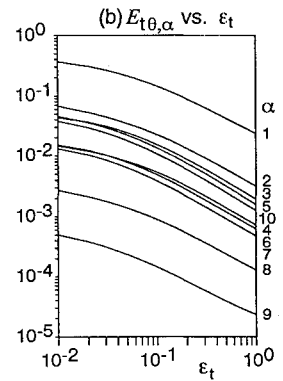


Fig. 5b Norms of the tip modal coefficients vs. payload size.

although keeping the payload characteristics unchanged. The quantities $E_{t\rho,\alpha}$ are plotted vs ε_0 in Fig. 5a for the first 10 vibration modes. The general tendency of these quantities to diminish with increasing spacecraft size is evident, and the rotational quantities $E_{b\rho,\alpha}$ showed similar behavior.

For the next case, we replace the payload mass matrix \mathbf{M}_l with $\varepsilon_l \mathbf{M}_l$ and vary ε_l although not tampering with the Shuttle mass characteristics. The variation of $E_{t\theta,\alpha}$ vs ε_0 is depicted in Fig. 5b for the given configuration. The curves for $E_{b\theta,\alpha}$ are similar. Extrapolating the curves, the main result of lemma 1 is seen to hold when the payload is much more massive than the manipulator. For the nominal payload ($\varepsilon_l = 1$), the vectors $\mathbf{J}_\theta \boldsymbol{\theta}_\alpha$ and $-\mathbf{J}_e \mathbf{q}_{e\alpha}$ agree to within 3% for all vibration modes in both translation and rotation. Most modes exhibit significantly better agreement than this ceiling formed by the first mode. From the graphs, it would appear that, asymptotically, $E_{t\rho,\alpha} \propto 1/\varepsilon_0$ and $E_{t\theta,\alpha} \propto 1/\varepsilon_l$ with similar comments holding true for the rotational components.

The key result underpinning the nonlinear analysis was given in Eq. (48). We shall compare its behavior with the exact values of $\mathbf{q}_e(t)$ generated by simulation. The model is subjected to control torques $\boldsymbol{\tau}(t)$ and spacecraft forces $\mathbf{f}_{0,c}(t)$ which are determined using the inverse dynamics equations for the rigid model of the system, with the prescribed joint angles parametrized by

$$\theta_n(t) = (\theta_{nT} - \theta_{n0}) \left(\frac{t}{T} - \frac{1}{2\pi} \sin \frac{2\pi t}{T} \right) + \theta_{n0} \quad n = 1, \dots, 6$$

where $\theta_{nT} \equiv 0.5$ rad, $\theta_{n0} \equiv 0.1$ rad ($n \neq 3$), and for $n = 3$, $\theta_{nT} = -0.5$ rad, $\theta_{n0} = -0.1$ rad. The desired spacecraft behavior is constant, i.e., $\rho_0(t) \equiv \mathbf{0}$. This trajectory for the duration time $T = 40$ s represents a generic rest-to-rest maneuver. A complete simulation code has been developed¹⁵ which uses a recursive Newton–Euler formulation of the motion equations to determine the accelerations $\ddot{\mathbf{q}}(t)$ which are integrated to produce $\dot{\mathbf{q}}(t)$ and $\mathbf{q}(t)$. All configuration dependencies as outlined in Sec. II are included as well as all nonlinearities which accrue from them. The geometric

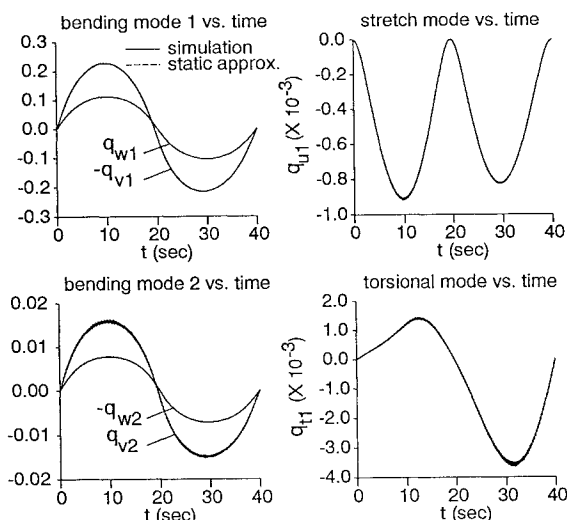


Fig. 6 Simulation and approximate values of the elastic coordinates (Link 2).

stiffening effect is captured using nonlinear strain-displacement relationships.²⁶

The exact values of $q_{2e}(t)$ generated by numerically integrating the motion equations are given in Fig. 6 along with those predicted by the approximation in Eq. (48). For the latter, we have suppressed the elastic dependence in the rigid and elastic Jacobian matrices so that only the joint angles generated by the simulation are used to update them. However, the simulation values of $q_e(t)$ are used to update the stiffness matrix. From the graphs, it is clear that the approximation holds quite accurately. Discrepancies between the two sets are not discernible from the plots and when the elastic dependence was incorporated into the Jacobians the agreement improved. The agreement obtained for the third link was very similar. It is worth mentioning the foreshortening of the link which is manifested by the stretch coordinate. It is a result of the coupling between bending and stretching which arises from inclusion of the geometric stiffening phenomenon. Note that the static approximation also captures the effect since it is due to nonlinearities in the stiffness matrix.

VI. Concluding Remarks

In this work, the important property of passivity in flexible space manipulator systems has been investigated. A very general analysis showed that the notion of reflected tip position can be extended to the multi-DOF case for space-based robots and that, in this noncollocated system, passivity is possible for massive payloads. This represents a significant extension of previous research which considered a pinned-free beam operating in the plane. Although the main results of the paper are approximate in nature, numerical examples showed them to hold quite accurately for a realistic model of a flexible 6-DOF manipulator carrying a large payload.

An added benefit of the approach taken here is an approximate static relationship between the applied torques and the discrete elastic coordinates. The elastic Jacobian matrix, in addition to determining the end-effector velocity, was shown to have an important role in this calculation. One of the difficulties in planning trajectories for flexible manipulators has been an a priori specification for the elastic coordinates. It is felt that the result presented here will be of some use in this regard. The linearized treatment of the motion equations yielded insight into the clamped-clamped behavior of the vibration modes.

Current research focuses on the exploitation of these results in the design of end-effector tracking controllers. Specifically, adaptive schemes which can handle large but otherwise uncertain payloads are being considered. Important in applications is the ability to synthesize the reflected tip position and its rates without measuring the elastic coordinates.

References

- Benhabib, R. J., Iwens, R. P., and Jackson, R. L., "Stability of Large Space Structure Control Systems Using Positivity Concepts," *Journal of Guidance, Control, and Dynamics*, Vol. 4, No. 5, 1981, pp. 487-494.
- Joshi, S. M., "Robustness Properties of Collocated Controllers for Flexible Spacecraft," *Journal of Guidance, Control, and Dynamics*, Vol. 9, No. 1, 1986, pp. 85-91.
- McLaren, M. D., and Slater, G. L., "Robust Multivariable Control of Large Space Structures Using Positivity," *Journal of Guidance, Control, and Dynamics*, Vol. 10, No. 4, 1987, pp. 393-400.
- Ortega, R., and Spong, M. W., "Adaptive Motion Control of Rigid Robots: A Tutorial," *Automatica*, Vol. 25, No. 6, 1989, pp. 877-888.
- Astrom, K. J., and Wittenmark, B., *Adaptive Control*, Addison-Wesley, Reading, MA, 1989, Chap. 4.
- Scott, M. A., Gilbert, M. G., and Demeo, M. E., "Active Vibration Damping of the Space Shuttle Remote Manipulator System," *Journal of Guidance, Control, and Dynamics*, Vol. 16, No. 2, 1993, pp. 275-280.
- Cannon, R. H., Jr., and Schmitz, E., "Initial Experiments on the End-Point Control of a Flexible One-Link Robot," *International Journal of Robotics Research*, Vol. 3, No. 3, 1984, pp. 62-75.
- Hughes, D., and Wen, J. T., "Passivity Motivated Controller Design for Flexible Structures," *Proceedings of the 1993 IEEE International Conference on Robotics and Automation* (Atlanta, GA), Vol. 3, Inst. of Electrical and Electronics Engineers, 1993, pp. 749-754.
- Barbieri, E., "Single-Input/Single-Output Transfer Functions for a Flexible Slewing Link," *Journal of Robotic Systems*, Vol. 10, No. 7, 1993, pp. 913-929.
- Wang, D., and Vidyasagar, M., "Transfer Functions for a Single Flexible Link," *International Journal of Robotics Research*, Vol. 10, No. 5, 1991, pp. 540-549.
- Pota, H. R., and Vidyasagar, M., "Passivity of Flexible Beam Transfer Functions with Modified Outputs," *Proceedings of the 1991 IEEE International Conference on Robotics and Automation* (Sacramento, CA), Inst. of Electrical and Electronics Engineers, 1993, 1991, pp. 2826-2831.
- Wang, D., and Vidyasagar, M., "Passive Control of a Stiff Flexible Link," *International Journal of Robotics Research*, Vol. 11, No. 6, 1992, pp. 572-578.
- Sincarsin, G. B., and Hughes, P. C., "Dynamics of Elastic Multibody Chains: Part A—Body Motion Equations," *Dynamics and Stability of Systems*, Vol. 4, Nos. 3 and 4, 1990, pp. 209-226.
- Hughes, P. C., and Sincarsin, G. B., "Dynamics of Elastic Multibody Chains: Part B—Global Dynamics," *Dynamics and Stability of Systems*, Vol. 4, Nos. 3 and 4, 1990, pp. 227-243.
- Damaren, C. J., and Sharf, I., "Simulation of Flexible-Link Manipulators with Inertial and Geometric Nonlinearities," *ASME Journal of Dynamic Systems, Measurement, and Control* (to be published).
- Hablani, H. B., "Hinges-Free and Hinges-Locked Modes of a Deformable Multibody Space Station—A Continuum Analysis," *Journal of Guidance, Control, and Dynamics*, Vol. 13, No. 2, 1990, pp. 286-296.
- Anderson, B. D. O., and Vongpanitlerd, S., *Network Analysis and Synthesis*, Prentice-Hall, Englewood Cliffs, NJ, 1973, Chaps. 2, 5.
- Papadopoulos, E., and Dubowsky, S., "On the Nature of Control Algorithms for Free-Floating Space Manipulators," *IEEE Transactions on Robotics and Automation*, Vol. 7, No. 6, 1991, pp. 750-758.
- Lozano-Leal, R., and Joshi, S. M., "On the Design of Dissipative LQG-Type Controllers," *27th IEEE Decision and Control Conference* (Austin, TX), Inst. of Electrical and Electronics Engineers, 1993, Vol. 2, 1988, pp. 1645-1646.
- Lanari, L., and Wen, J. T., "Asymptotically Stable Set Point Control Laws for Flexible Robots," *Systems and Control Letters*, Vol. 19, July-Aug. 1992, pp. 119-129.
- Desoer, C. A., and Vidyasagar, M., *Feedback Systems: Input-Output Properties*, Academic Press, New York, 1975, Chap. 6.
- Vidyasagar, M., *Nonlinear Systems Analysis*, 2nd ed., Prentice-Hall, Englewood Cliffs, NJ, 1993, Chap. 6.
- Willems, J. C., "Dissipative Dynamical Systems, Part I: General Theory; Part II: Linear Systems with Quadratic Supply Rates," *Archive for Rational Mechanics and Analysis*, Vol. 45, July 1972, pp. 321-393.
- Zames, G., "On the Input-Output Stability of Time-Varying Nonlinear Feedback Systems, Part I: Conditions Derived Using Concepts of Loop Gain, Conicity, and Positivity; Part II: Conditions Involving Circles in the Frequency Plane and Sector Nonlinearities," *IEEE Transactions on Automatic Control*, Vol. AC-11, No. 2, 1966, pp. 228-238, 465-476.
- Hill, D. J., and Moylan, P. J., "Stability Results for Nonlinear Feedback Systems," *Automatica*, Vol. 13, July 1977, pp. 377-382.
- Hanagud, S., and Sarkar, S., "Problem of the Dynamics of a Cantilevered Beam Attached to a Moving Base," *Journal of Guidance, Control, and Dynamics*, Vol. 12, No. 3, 1989, pp. 438-441.